ARTICLE

OBC
www.rsc.org/obc

Solvent affects the conformation of virginiamycin M_1 (pristinamycin IIA, streptogramin A)†

Jason Dang,[a] Mikael Bergdahl,[b] Frances Separovic,[c] Robert T. C. Brownlee[d] and Robert P. Metzger*[e]

[a] *School of Chemistry, LaTrobe University, VIC 3086 Australia. E-mail: j.dang@latrobe.edu.au; Fax: +61 3 9479 1399; Tel: +61 3 9479 2582*

[b] *Department of Chemistry and Biochemistry, San Diego State University, San Diego, CA 92182-1030, USA. E-mail: bergdahl@sciences.sdsu.edu; Fax: +01 619 594 4634; Tel: +1-619 594 5865*

[c] *School of Chemistry, The University of Melbourne, VIC 3010 Australia. E-mail: fs@unimelb.edu.au; Fax: +61 3 9347 5180; Tel: +61 3 8344 6464*

[d] *School of Chemistry, LaTrobe University, VIC 3086 Australia. E-mail: r.brownlee@latrobe.edu.au; Fax: +61 3 9479 1399; Tel: +61 3 9479 2547*

[e] *Department of Chemistry and Biochemistry, San Diego State University, San Diego, CA 92182-1030, USA. E-mail: rmetzger@sciences.sdsu.edu; Fax: +1 619 594 4634; Tel: +1 619 594 6801*

Received 25th May 2004, Accepted 16th August 2004
First published as an Advance Article on the web 16th September 2004

The streptogramins are antibiotics which act by binding two different components at separate nearby sites on the bacterial 50S ribosome, inhibiting protein synthesis. The first component, a macrolactone, is common to many of the streptogramin antibiotics and, thus, is referred to by many names including virginiamycin M_1 (VM1), pristinamycin IIA, ostreogrycin A and streptogramin A. X-Ray crystallographic studies of VM1 bound to ribosomes and to a deactivating enzyme show a different conformation to that of VM1 in chloroform solution. We now report the results of high resolution 2D NMR experiments that show that the conformation of VM1 in dimethyl sulfoxide and methanol differs from both that in chloroform solution and in the bound form. The 3D structure and the ^{1}H NMR and ^{13}C NMR chemical shifts of VM1 in dimethyl sulfoxide and methanol are described.

Introduction

Virginiamycin is one of a number of streptogramin antibiotics produced by several species of *Streptomyces.* First reported in 1955,[1] virginiamycin was soon found to be a mixture of similar compounds with the major components being the macrolactone virginiamycin M_1 and the hexadepsipeptide virginiamycin S_1.[2–4] Indeed, all of the *Streptomyces*-derived antibiotics are composed of the same macrolactone component and slightly different hexadepsipeptide components.[3,4] As a result, the common macrolactone component appears in the literature under several names, *viz.* virginiamycin M_1, pristinamycin IIA, ostreogrycin A, streptogramin A, PA 114 A1, vernamycin A, staphylomycin M_1, synergistin A1 and mikamycin A.[3,4] Indeed, it was as ostreogrycin A in 1966 that the completed chemical structure of virginiamycin M_1, shown in Fig. I, was announced.[5,6] In this paper, we shall refer to the macrolactone compound of the antibiotic as virginiamycin M_1 or VM1 and use the term B component for hexadepsipeptide components when not referring to a specific compound.

The B components and VM1 affect primarily Gram-positive bacteria. Administered individually, they are bacteriostatic but they interact synergistically to have a bactericidal effect on susceptible bacteria,[4,7] known since 1961 to be the result of inhibition of bacterial protein synthesis.[8] In 1965, the first report that VM1 and the B components inhibited protein synthesis by binding to bacterial ribosomes appeared.[9] Indeed, VM1 binds to 50S ribosomes isolated from Gram-positive and Gram-negative bacteria, 60S animal and yeast ribosomes[10] and animal mitochondrial 55S ribosomes,[11] with protein synthesis inhibition correlated with antibiotic ribosomal binding strength. In 1978, virginiamycin S_1 was reported to bind to 50S bacterial ribosomes with a resultant change in its fluorescence spectrum.[12] The binding and mechanism of protein inhibition is the subject of many subsequent reports, culminating in the understanding that the B component affects the protein exit path of the 50S ribosomal subunit.[13] Recent reports have reported the elucidation of the nucleotide bases affected by VM1 binding at its site on the 23S rRNA component of the 50S ribosome[14] and, in a scientific *tour de force*, the actual visualization of the VM1 bound to a specific site on the 50S ribosome by X-ray crystallographic methods.[15]

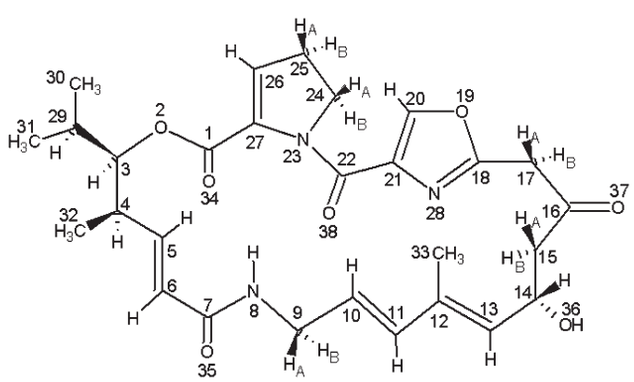

Fig. 1 The chemical structure and numbering of virginiamycin M_1 (VM1) {virginiamycin M_1 (CA: 21411-53-0) with IUPAC name: {8,9,14,15,24,25-hexahydro-14-hydroxy-4,12-dimethyl-3-(1-methylethyl)-(3*R*,4*R*,5*E*,10*E*,12*E*,14*S*)-3*H*-21,18-nitriolo-1*H*,22*H*-pyrrolo-[2,1-*c*][1,8,4,19]-dioxadiazacyclotetracosine-1,7,16,22(4*H*,17*H*)-tetrone}.

The crystal structure of the 50S ribosomes with bound VM1[15] (PDB ID 1N8R) as well as the crystal structure of VM1 bound to Vat(D)[16](PDB ID 1KHR), a streptogramin acetyl-S-coenzyme A acetyltransferase, yield essentially the same VM1 conformation. The conformation in chloroform

† Electronic supplementary information (ESI) available: solution structures of virginiamycin in dimethyl sulfoxide, methanol and chloroform. See http://www.rsc.org/suppdata/ob/b4/b407724e/

DOI: 10.1039/b407724e

Table 1 ^{13}C and ^{1}H NMR chemical shifts obtained in d_6-DMSO at 30 °C. Most values are averages of data obtained using 500 and 400 MHz NMR spectrometers[a] with the range in values shown. *J* values that could be determined reliably are also shown

Position	δ_C (ppm)	$\Delta(\delta_C)$ range	δ_H (ppm)	$\Delta(\delta_H)$ range	m	*J*/Hz	*J*/Hz	*J*/Hz
1	160.02	0.03						
3	79.99	0.01	4.77	0.02	dd	$^3J_{3,29} = 10$	$^3J_{3,4} = 2$	
4	36.51	0.02	2.73	[a]	m			
5	143.29	0.08	6.57	0.02	dd	$^3J_{5,6} = 16$	$^3J_{5,4} = 7$	
6	124.66	0.01	5.89	0.02	dd	$^3J_{6,5} = 16$		
7	164.96	0.03						
8 (N)			7.75	0.00	bt	$^3J_{8,9} = 2$	$^3J_{8,9'} = 4$	
9A	39.36	[a]	3.71	[a]	m	$^2J_{9A,9B} = 18$		
9B	39.36	[a]	4.02	[a]	m	$^2J_{9B,9A} = 18$		
10	125.67	0.05	5.53	0.02	ddd	$^3J_{10,11} = 16$	$^3J_{10,9B} = 3$	$^3J_{10,9} = 7$
11	133.66	0.05	5.85	0.01	d	$^3J_{11,10} = 16$		
12	132.41	0.03						
13	133.03	0.05	5.03	0.01	d	$^3J_{13,14} = 9$		
14	63.68	0.01	4.67	0.02	ddd	$^3J_{14,13} = 9$	$^3J_{14,15B} = 9$	$^3J_{14,15A} = 4$
15A	49.31	0.04	2.69	[a]	m			
15B	49.31	0.04	2.97	0.02	dd	$^2J_{15B,15A} = 14$	$^3J_{15B,14} = 9$	
16	201.42	0.09						
17A	43.66	0.00	3.76	0.02	d	$^2J_{17A,17B} = 16$		
17B	43.66	0.00	4.12	0.02	d	$^2J_{17B,17A} = 16$		
18	157.28	0.05						
20	145.04	0.04	8.51	0.01	s			
21	135.35	0.02						
22	159.91	0.03						
24A	50.66	0.06	4.03	[a]	m			
24B	50.66	0.06	4.15	[a]	m			
25A	29.65	0.04	2.65	[a]	m			
25B	29.65	0.04	2.73	[a]	m			
26	125.33	0.17	6.27	0.01	dd	$^3J_{26,25A} = 3$	$^3J_{26,25B} = 3$	
27	136.07	−0.02						
29	29.18	0.02	1.93	0.02	m			
30	19.28	0.05	0.94	0.02	d	$^3J_{30,29} = 7$		
31	18.72	0.02	0.87	0.02	d	$^3J_{31,29} = 7$		
32	11.82	0.00	1.05	0.02	d	$^3J_{32,4} = 7$		
33	12.52	0.04	1.57	0.02	s			
36 (O)			4.12	[a]				

[a] Values from only one instrument were used because 2D NMR data were needed to resolve peaks.

solution differs significantly from the bound form, as shown by recent high resolution studies of VM1,[17] which confirm the earlier conformations of VM1 determined by small molecule X-ray crystallography[18] and NMR studies in chloroform solution.[19,20] Evidently VM1 changes its conformation as it passes from solution to the form bound to ribosome or enzyme active sites. Chloroform solution could be taken as a model system for VM1 in a hydrophobic environment, but VM1 will appear in aqueous as well as hydrophobic environments during transport to and within the bacterial cell. Knowledge of VM1 conformations in different solvents is needed to more fully understand the mechanism of its antibiotic action, especially details of the conformational changes in the binding process itself.

The limited solubility of VM1 in water[21] precludes 2D NMR experiments allowing determination of its conformation in aqueous solution. However, it might be possible to infer the aqueous conformation of VM1 by considering its conformation in representative solvents in addition to chloroform. In this paper, we report that there are different conformations of VM1 in chloroform, methanol and dimethyl sulfoxide as determined by 1D and 2D NMR experiments, including COSY, TOCSY, HMQC, HMBC, ROESY and NOESY experiments. We use these results and 1D NMR experiments with VM1 in deuterium oxide and deuterium oxide–methanol mixtures to propose a conformation for VM1 in water.

Results

NMR assignments for VM1

Fig. 2 depicts typical 1D ^1H NMR of VM1 in d_6-DMSO and in CD_3OD solutions with the NMR resonances clearly identified. Similar 1D and 2D NMR spectra were obtained for VM1 in $CDCl_3$,[17] CD_3OD and d_6-DMSO solvents. The proton shifts for VM1 in $CDCl_3$ did not differ significantly at temperatures of 20, 25, 30 and 40 °C implying no temperature dependent conformational changes.[17] Assignments were made using a combination of DEPT and 2D experiments and particularly using HMBC correlations to resolve any unambiguous assignments. The HMBC correlations for VM1 in d_6-DMSO and CD_3OD are depicted in Fig. 3A and 3B, respectively. The 1D ^1H-NMR spectra for VM1 in D_2O and in CD_3OD–D_2O mixtures were also similar to that of Fig. 2. Tables 1 and 2 show complete proton and carbon chemical shift assignments for VM1 in these various solvents.

Solvent effect on chemical shifts

ROESY and NOESY data were collected separately in CD_3OD and d_6-DMSO for use in determining the 3D structures of VM1. As expected for a molecule of this size,[22,23] the ROESY experiments yielded more correlations and were used for subsequent work. Fig. 3(C&D) depicts the principal long-range connectivities for those experiments performed in d_6-DMSO and CD_3OD. Chemical shift for H-8, H-17A and H-17B, identified as exchangeable with deuterium in acidified $CDCl_3$ by Kingston *et al.*,[6] slowly disappeared when VM1 in CD_3OD solutions were employed in the experiments. This will be reported in detail in a subsequent publication.

3D structures

The ROESY 2D NMR data were used to generate the conformations shown in Fig. 4 for d_6-DMSO, and CD_3OD solutions. Also depicted in Fig. 4 is the 3D structure of VM1 bound to the 50S ribosome, as taken from the X-ray crystallographic data of Hansen *et al.*,[15] in the Protein Data Bank (PDB ID 1N8R) and of VM1 in chloroform reported by Dang *et al.*[17]

The energy-minimized structures for VM1 in $CDCl_3$, d_6-DMSO and CD_3OD with distinct different conformations in

Table 2 ^{13}C and ^{1}H NMR chemical shifts obtained in CD_3OD at 30 °C. Most values are averages of data obtained using 500 and 400 MHz NMR spectrometers[a] with the range in values shown. *J* values that could be determined reliably are also shown[b]

Position	δC (ppm)	$\Delta(\delta_C)$ range	#H/C	δ_H (ppm)	$\Delta(\delta_H)$ range	m	*J*/Hz	*J*/Hz	*J*/Hz
1	160.02	0.03	0						
3	79.99	0.01	1	4.77	0.02	dd	$^3J_{3,29} = 10$	$^3J_{3,4} = 2$	
4	36.51	0.02	1	2.73	[a]	m			
5	143.29	0.08	1	6.57	0.02	dd	$^3J_{5,6} = 16$	$^3J_{5,4} = 7$	
6	124.66	0.01	1	5.89	0.02	d	$^3J_{6,5} = 16$		
7	164.96	0.03	0						
8 (N)				7.75	0.00	dd	$^3J_{8,9} = 2$	$^3J_{8,9'} = 4$	
9A	39.19	0.35	2	3.71	[a]	m			
9B	39.19	0.35	2	4.02	[a]	m			
10	125.67	0.05	1	5.53	0.02	ddd	$^3J_{10,11} = 16$	$^3J_{10,9B} = 4$	$^3J_{10,9} = 6$
11	133.66	0.05	1	5.85	0.01	d	$^3J_{11,10} = 16$		
12	132.41	0.03	0						
13	133.03	0.05	1	5.03	0.01	d	$^3J_{13,14} = 9$		
14	63.68	0.01	1	4.67	0.02	ddd	$^3J_{14,13} = 9$	$^3J_{14,15B} = 9$	$^3J_{14,15A} = 5$
15A	49.31	0.04	2	2.69	[a]	m			
15B	49.31	0.04	2	2.97	0.02	dd	$^2J_{15B,15A} = 14$	$^3J_{15B,14} = 9$	
16	201.42	0.09	0						
17A	43.66	0.00	2	3.76	0.02	d	$^2J_{17A,17B} = 16$		
17B	43.66	0.00	2	4.12	0.02	d	$^2J_{17B,17A} = 16$		
18	157.28	0.05	0						
20	145.04	0.04	1	8.51	0.01	s			
21	135.35	0.02	0						
22	159.91	0.03	0						
24A	50.66	0.06	2	4.03	[a]	m			
24B	50.66	0.06	2	4.15	[a]	m			
25A	29.65	0.04	2	2.65	[a]	m			
25B	29.65	0.04	2	2.73	[a]	m			
26	125.33	0.17	1	6.27	0.01	t	$^3J_{26,25A} = 3$	$^3J_{26,25B} = 3$	
27	136.07	0.02	0						
29	29.18	0.02	1	1.93	0.02	m			
30	19.28	0.05	3	0.94	0.02	d	$^3J_{30,29} = 7$		
31	18.72	0.02	3	0.87	0.02	d	$^3J_{31,29} = 6$		
32	11.82	0.00	3	1.05	0.02	d	$^3J_{32,4} = 7$		
33	12.52	0.04	3	1.57	0.03	s			

[a] Values from only one instrument were used; either because 2D NMR data was needed to resolve peaks or as a result of signal loss due to exchange reactions (proton resonances at H-8, H- 17A and 17B were gradually lost). [b] Preliminary data showed *J* values obtained in D_2O and CD_3OD mixtures were similar to the values reported here. The H–D exchange, D_2O and D_2O–CD_3OD results will be reported in more detail in a subsequent publication.

Table 3 Comparison of the 20 energy-minimized NMR structures of VM1 in solvent and the X-ray crystal structure[a]

Conformational energy	$CDCl_3$	DMSO	CD_3OD	X-Ray
E_{total}/kcal mol^{-1}	43.54 ± 3.55	45.10 ± 3.88	35.60 ± 1.43	34.51
E_{NOE}/kcal mol^{-1}	12.21 ± 2.74	3.92 ± 1.67	7.60 ± 0.98	NA
E_{bond}/kcal mol^{-1}	8.33 ± 0.37	7.81 ± 0.18	7.99 ± 0.22	8.11
E_{phi}/kcal mol^{-1}	21.64 ± 4.90	30.60 ± 2.63	19.85 ± 0.57	18.99
$E_{repulsion}$/kcal mol^{-1}	129.26 ± 2.31	132.51 ± 2.27	125.42 ± 1.29	127.39
$E_{dispersion}$/kcal mol^{-1}	−112.58 ± 3.56	−119.55 ± 2.49	−110.50 ± 1.34	−109.55
Average of the global backbone RMSD[a]	0.29 ± 0.14	0.53 ± 0.22	0.39 ± 0.34	

[a] RMSD calculated using MOLMOL Program.

each solvent are shown in Fig. 5. The most striking change between the different conformations is that the planes of the oxazole and proline rings rotate to a different degree both relative to the molecule framework and to one another in each solvent.

Table 3 compares the calculated total energies of the structures that were derived for each solvent system and for the X-ray structure. It is clear that this molecule has a range of conformations of similar energy, which are stabilized by a combination of molecular–solvent interactions and variation in internal forces within the molecule. Also shown are the energy contributions to this calculated total energy, and the additional energy of the molecule with the NOE constraints included.

Fig. 6 shows the average conformation of VM1 in the three solvents. It is clear from both Figs. 5 and 6 that the structure in CD_3OD is significantly different from that of the other two solvents. In both the $CDCl_3$ and the DMSO structures there is an internal hydrogen bond between the VM1 C14 hydroxyl group and O37, the oxygen of the C16 carbonyl group which constraints the 'western end' of the molecule (right hand-side of Fig. 1). In CD_3OD this hydrogen bond is not present: presumably the C14 hydroxyl group and the carbonyl O37 are hydrogen bonded to the solvent, removing this constraint and resulting in a different structure, more closely related to that seen in VM1 bound to Vat(D). This process may be important for biological activity.

Discussion

From Figs. 4–6, it is obvious that the solvent has influence on the overall conformation of VM1. As can be seen in Fig. 6, VM1 has a flatter globular structure in d_6-DMSO, a slightly twisted structure in CD_3OD and a 'C' or grooved shape in $CDCl_3$. As a result different functional groups are extended and VM1 may exhibit solvent-dependent binding properties. This behaviour could be anticipated in that hydrophobic solvents such as $CDCl_3$ might be expected to force the hydrophilic groups of

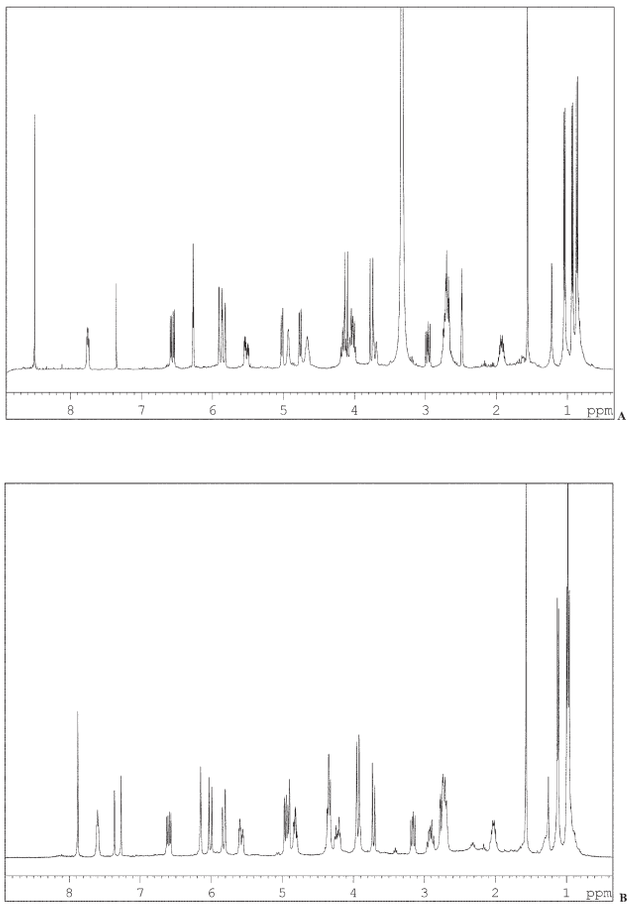

Fig. 2 ^{1}H NMR spectra of VM1 in: (a) d_6-DMSO, and (b) $CDCl_3$ acquired at 30 °C and 400 MHz. Experimental conditions are described in the text.

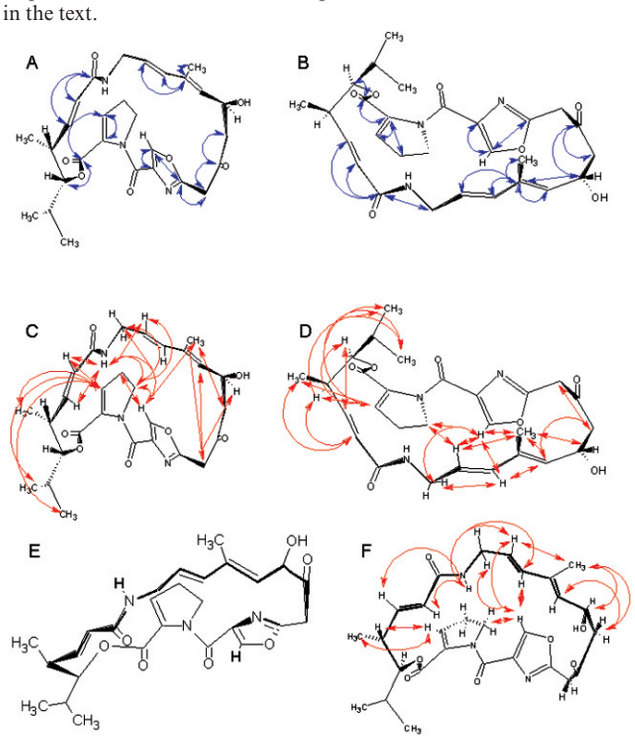

Fig. 3 Depictions of the conformation of virginiamycin M_1: (A) in d_6-DMSO solution showing HMBC connectivities to quaternary centres, (B) in CD_3OD solution showing HMBC connectivities to quaternary centres, (C) in d_6-DMSO solution illustrating the principal long-range ROESY connectivities observed, (D) in CD_3OD solution illustrating the principal long-range ROESY connectivities observed, (E) a representation of VM1 bound to the 50S-ribosome,[15] and (F) in $CDCl_3$.[17] Heavier lines indicate bonds facing outward; lighter lines indicate bonds inside the ring. Both models are consistent with the chirality (3*R*,4*R*,14*S*) found in the X-ray crystal structure of the ribosomal and the Vat(D) bound VM1[15,16] as discussed further in the text.

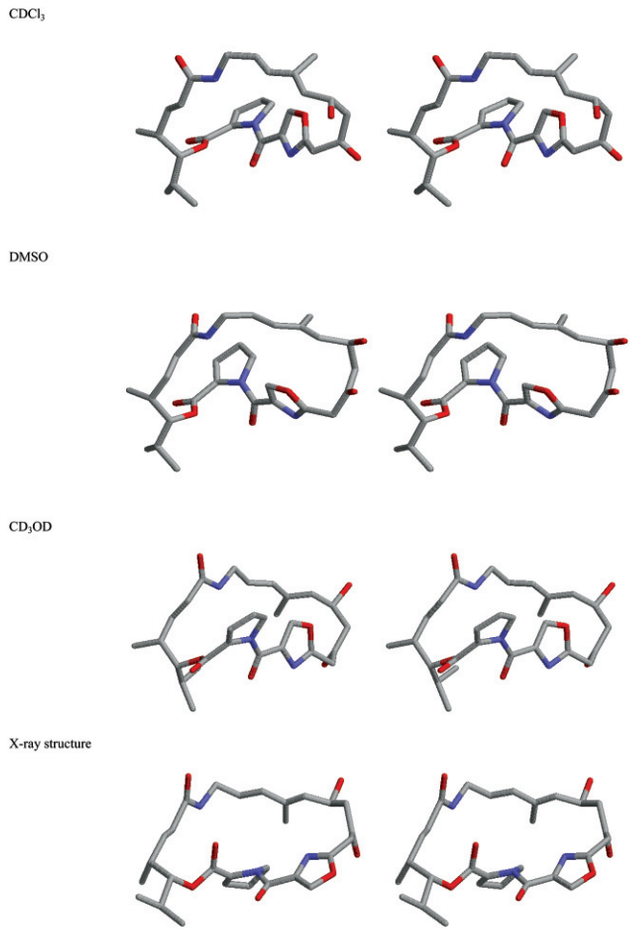

Fig. 4 Comparison of the conformation of VM1 in $CDCl_3$, d_6-DMSO and CD_3OD based on NMR experiments (average conformation of the 20 structures shown in Fig. 5) and the X-ray structure of Hansen *et al.*[15] Stereo diagrams of the molecules are shown to illustrate the orientation of the rings.

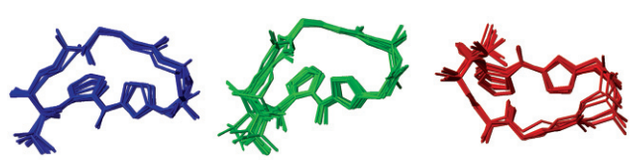

Fig. 5 20 energy-minimized structures of VM1 in $CDCl_3$ (blue), d_6-DMSO (green), and CD_3OD (red).

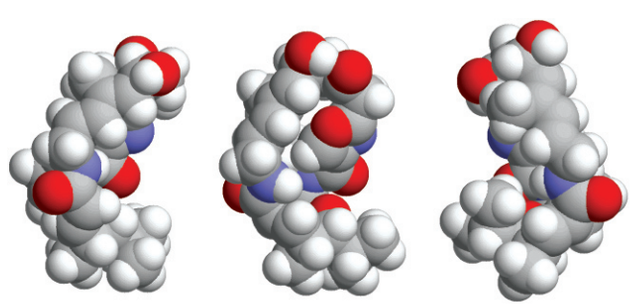

Fig. 6 Comparison of VM1 structures in the three solvents shown as space-filling surfaces. The conformations assumed by VM1 in $CDCl_3$ (left), d_6-DMSO (center) and CD_3OD (right) are distinctly different. Note the hydrogen bonding between the C14 hydroxyl group and the C-16 carbonyl oxygen in $CDCl_3$ and d_6-DMSO, but not CD_3OD. The structures are shown in an orientation to highlight similarities between them.

the molecule into the interior to interact with other hydrophilic groups on the opposing part of the ring. Conversely, exposure to more hydrophilic solvents might be expected to force more hydrophobic parts of the molecule inward, leaving hydrophilic parts facing outward. The conformations of VM1 in the solvents are more compact than that of the form bound

to the 50S ribosome (Fig. 4D) or to the active site of Vat(D). Indeed, VM1 bound to either ribosome or enzyme is flattened and spread out almost to the maximum extent, undoubtedly aided by hydrophobic and polar interactions between molecular groups and the binding sites.[15,16] In the acetyltransferase, the bound conformation places the C-14 hydroxyl group into a position close to the acetyl group that will acetylate the VM1.[16] In the 50S ribosome, the bound conformation enables VM1 to cover and interact with both the A and P sites leading to a conformational change which leads to enhanced binding of a streptogramin B component, which then act synergistically to cause loss of ribosomal peptide synthesis activity.[13,15] The change in conformation exhibited by VM1 in different solvents indicates the flexibility in this relatively small cyclic molecule and allude to possible changes in conformation that may be important to its antibiotic activity.

Materials and methods

Chemicals

Deuterated chloroform ($CDCl_3$), methanol (CD_3OD and CD_3OH), d_6-dimethyl sulfoxide (d_6-DMSO) and deuterium oxide (D_2O) were obtained from Aldrich (Milwaukee, USA). Silica gel was obtained from Whatman (Maidstone, UK). Methanol, benzene and dichloromethane were purchased from Fisher scientific (ACS reagent grade, USA) and used directly without purification.

Virginiamycin M_1 and S_1 were extracted from Stafac® pig feed containing 4% virginiamycins (Pfizer, USA) by using a modification of the procedure of Sharma *et al.*[24] 125 g Stafac® were mixed with 1 L 50% methanol in dichloromethane, stirred and allowed to settle for 30 min. before removal of the solid material by filtration. The solvent was removed *in vacuo* to give 16 g crude material of the antibiotics. The solid material was taken up in 10% methanol in dichloromethane and applied on a flash silica gel (60 Å, 230–400 mesh) column (25 cm × 5 cm) and separate fractions of virginiamycins M_1 and S_1 were eluted using the same solvent. The identity and purity of the virginiamycin fractions were assessed with TLC in 10% methanol in dichloromethane (R_f VM1 ~ 0.4; R_f virginiamycin S_1 ~ 0.3, detected with a UV lamp) and by ^{1}H-NMR.

The VM1 preparation was subsequently recrystallized from 10% methanol in dichloromethane. The recrystallized VM1 was further dried using a Dean–Stark setup with benzene as a solvent. After benzene removal, 1.8 g of pure light yellow colored VM1 was obtained along with 250 mg pure virginiamycin S_1.

NMR experiments

NMR experiments were performed on Varian Inova 400 MHz and 500 MHz NMR spectrometers (Varian Inc, Palo Alto, CA) and a Bruker (Karlsruhe, Germany) AVANCE DRX 400 MHz NMR spectrometer. Spectra were recorded in deuterated solvents: $CDCl_3$, d_6-DMSO, CD_3OD, CD_3OH and, in preliminary experiments, D_2O and CD_3OD–D_2O (1 : 1) mixtures. The chemical shifts were referenced relative to an appropriate solvent peak and tetramethylsilane (TMS) set to 0.0 ppm. 1D ^{1}H, ^{13}C, and DEPT experiments were carried out using standard protocols.[22,23,25] 2D NMR spectra including COSY and TOCSY were acquired and processed using standard protocols.[22,23,25] 2D ^{1}H NMR nuclear Overhauser enhancement spectroscopy (NOESY)[22,23,25] and ROESY spectra[26,27] were recorded in CD_3OD, $CDCl_3$ and d_6-DMSO at 400 MHz using a 2.5 s relaxation delay and 300 ms mixing time with a spectral width of 4.5 kHz in each dimension, 2048 complex data points in F2, 448 increments and 32 transients per increment and Fourier transforming to 2048 and 1024 in F2 and F1, respectively. For TOCSY spectra, a 50 ms mixing time in CD_3OD and $CDCl_3$ and 160 ms in d_6-DMSO were used.

All 2D NMR spectra were processed using the Bruker XWIN-NMR package A QSINE function with $\pi/2$ shift was used for the NOESY spectra in both dimensions and zero filling was used to double the number of points in the FID. The spectra were analyzed with the XEASY[28] software for chemical shift and NOE attributions. We have used the $H15_{AB}$ NOE, corresponding to a distance of 1.79 Å, to calibrate the NOEs of the non-aromatic protons. A 60% error was applied to the peak integration for all distance constraint calculations.

Structures were generated by simulated annealing carried out using DYANA.[29] 200 structures were calculated from an extended structure using a torsion mode, 47 distance constraints, derived from 25 sequential, 8 long-range, 9 medium-range and 5 cyclic linkage and 48 NOE-based distance constraints for VM1 in $CDCl_3$ and DMSO, respectively.

Dynamics and energy calculations were performed using Insight and Discover software[30] using the CVFF forcefield. 20 structures that satisfied the experimental constraints with violations less than 0.5 Å were select as starting conformation for molecular dynamics. High-temperature steps were used (1.0 fs) up to a final temperature of 900 K then cooling down to 195 K was applied. Finally, steepest descent and conjugated gradient minimization steps were performed until 0.0001 derivatives were reached. The structures presented in this work include the 20 lowest total energy structures selected from the 200 structural calculations according to the NOE and overall energies. The software package MOLMOL[31] was used to visualize the calculated structures and compute the RMSD data.

Acknowledgements

We thank Dr LeRoy Lafferty (SDSU) for his assistance in obtaining the 500 MHz NMR spectra.

References

1 P. De Somer and P. Van Dijck, *Antibiot. Chemother. (Basel)*, 1955, **5**, 632–639.
2 H. Vandehaeghe, P. Van Dijck, G. Parmentier and P. De Somer, *Antibiot. Chemother. (Basel)*, 1957, **7**, 606–614.
3 P. Crooy and R. De Neys, *J. Antibiot.*, 1972, **25**, 371–372.
4 G. Bonfiglio and P. M. Furneri, *Expert Opin. Ther. Pat.*, 2003, **13**, 651–659.
5 G. R. Delpierre, F. W. Eastwood, G. E. Gream, D. G. I. Kingston, P. S. Sarwin, Lord Todd and D. H. Williams, *J. Chem. Soc. C*, 1966, 1653–1699.
6 D. G. I. Kingston, Lord Todd and D. H. Williams, *J. Chem. Soc. C*, 1966, 1669–1676.
7 P. Van Dijck, H. Vandehaeghe and P. De Somer, *Antibiot. Chemother.*, 1957, **7**, 625–629.
8 H. Yamaguchi, *J. Antibiot.*, 1961, **14**, 313–328.
9 H. L. Ennis, *J. Bacteriol.*, 1965, **90**, 1109–1119.
10 D. Vazquez, E. Battaner, R. Neth, G. Heller and R. E. Monro, *Cold Spring Harbor Symp. Quant. Biol.*, 1969, **XXXIV**, 369–375.
11 N. R. Towers, G. M. Kellerman and A. W. Linnane, *Arch. Biochem. Biophys.*, 1973, **155**, 159–166.
12 B. Parfait, M. P. De Béthune and C. Cocito, *Mol. Gen. Genet.*, 1978, **166**, 45–51.
13 T. Tenson, M. Lovmar and M. Ehrenberg, *J. Mol. Biol.*, 2003, **330**, 1005–1014.
14 B. T. Porse and R. A. Garrett, *J. Mol. Biol.*, 1999, **286**, 375–387.
15 J. L. Hansen, P. B. Moore and T. A. Steitz, *J. Mol. Biol.*, 2003, **330**, 1061–1075.
16 M. Sugantino and S. L. Roderick, *Biochemistry*, 2002, **41**, 2209–2216.
17 J. Dang, B. M. Bergdahl, F. Separovic, R. T. C. Brownlee and R. P. Metzger, *Aust. J. Chem.*, 2004, **57**, 415–418.
18 P. Durant, G. Evrard, J. P. Declercq and G. Germain, *Cryst. Struct. Commun.*, 1974, **3**, 501–510.
19 B. W. Bycroft, *J. Chem. Soc., Perkin Trans. 1*, 1977, 2464–2470.
20 E. Surcouf, I. Morize, D. Frechet, M. Vuilhorgne, A. Mikou, E. Guitet and J. Y. Lallemand, *Stud. Phys. Theor. Chem.*, 1990, **71**, 719–726.
21 J. M. Paris, J. C. Barrière, C. Smith and P. E. Bost, in G. Lukacs and M. Ohno, editors, *Recent Progress in the Chemical Synthesis of Antibiotics*, Springer-Verlag, Berlin, Heidelberg, NY, London, Paris, Tokyo, Hong Kong, Barcelona, 1990, pp. 183–248.
22 R. R. Ernst, G. Bodenhausen and A. Wokaun, *Principles of Nuclear Magnetic Resonance in One and Two Dimensions*, Clarendon Press, Oxford, UK, 1987.

23 T. D. W. Claridge, *High-Resolution NMR Techniques in Organic Chemistry*, Pergamon Press, New York, 1999.
24 N. K. Sharma, N. Hosten and M. J. O. Anteunis, *Bull. Soc. Chim. Belges*, 1988, **97**, 185–192.
25 S. Braun, H.-O. Kalinowski and S. Berger, *150 and More Basic NMR Experiments*, Wiley-VCH, Weinheim, Germany, 1998.
26 J. Jeener, B. H. Meier, P. Bachmann and R. R. Ernst, *J. Chem. Phys.*, 1979, **71**, 4546–4553.
27 S. Macura and R. R. Ernst, *Mol. Phys.*, 1980, **41**, 95–117.
28 C. Bartels, T. H. Xia, M. Billeter, P. Güntert and K. Wüthrich, *J. Biomol. NMR*, 1995, **5**, 1–10.
29 P. Güntert, C. Mumenthaler and K. Wüthrich, *J. Mol. Biol.*, 1997, **273**, 283–298.
30 Accelrys Inc., San Diego, 1999.
31 R. Koradi, M. Billeter and K. Wüthrich, *J. Mol. Graphics*, 1996, **14**, 51–55.